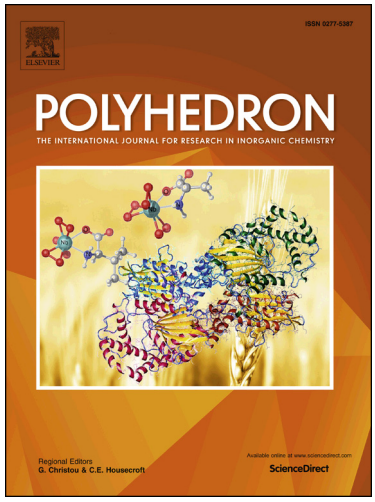

Synthesis, crystal structure, magnetic properties and DFT study of dinuclear Ni(II) complex with the condensation product of 2-quinolinecarboxaldehyde and Girard's T reagent

Mima Č. Romanović, Božidar R. Čobeljić, Andrej Pevec, Iztok Turel, Vojislav Spasojević, Arshak A. Tsaturyan, Igor N. Shcherbakov, Katarina K. Anđelković, Marina Milenković, Dušanka Radanović, Milica R. Milenković

PII: S0277-5387(17)30161-4
DOI: http://dx.doi.org/10.1016/j.poly.2017.02.039
Reference: POLY 12506

To appear in: *Polyhedron*

Received Date: 17 January 2017
Revised Date: 22 February 2017
Accepted Date: 27 February 2017

Please cite this article as: M.C. Romanović, B.R. Čobeljić, A. Pevec, I. Turel, V. Spasojević, A.A. Tsaturyan, I.N. Shcherbakov, K.K. Anđelković, M. Milenković, D. Radanović, M.R. Milenković, Synthesis, crystal structure, magnetic properties and DFT study of dinuclear Ni(II) complex with the condensation product of 2-quinolinecarboxaldehyde and Girard's T reagent, *Polyhedron* (2017), doi: http://dx.doi.org/10.1016/j.poly.2017.02.039

Synthesis, crystal structure, magnetic properties and DFT study of dinuclear Ni(II) complex with the condensation product of 2-quinolinecarboxaldehyde and Girard's T reagent

Mima Č. Romanović[a], Božidar R. Čobeljić[a], Andrej Pevec[b], Iztok Turel[b], Vojislav Spasojević[c], Arshak A. Tsaturyan[d], Igor N. Shcherbakov[d], Katarina K. Anđelković[a], Marina Milenković[e], Dušanka Radanović[f], Milica R. Milenković[a1]

[a]*Faculty of Chemistry, University of Belgrade, Studentski trg 12-16, 11000 Belgrade, Serbia*

[b]*Faculty of Chemistry and Chemical Technology, University of Ljubljana, Večna pot 113, 1000 Ljubljana, Slovenia*

[c]*Institute of Nuclear Sciences 'Vinča', Condensed Matter Physics Laboratory, P.O. Box 522, 11001 Belgrade, Serbia*

[d]*Department of Chemistry, Southern Federal University, Zorge St. 7, 344090, Rostov-on-Don, Russia*

[e]*Faculty of Pharmacy, Department of Microbiology and Immunology, University of Belgrade, Vojvode Stepe 450, 11221 Belgrade, Serbia*

[f]*Institute of Chemistry, Technology and Metallurgy, University of Belgrade, Njegoševa 12, P.O. Box 815, 11000 Belgrade, Serbia*

Abstract

A dinuclear double end-on azido bridged Ni(II) complex $[Ni_2\mathbf{L}_2(\mu\text{-}_{1,1}\text{-}N_3)_2(N_3)_2]$ (**1**) with the condensation product of 2-quinolinecarboxaldehyde and trimethylammonium acetohydrazide chloride (Girard's T reagent) (**HL**Cl) has been synthesized and characterized by elemental analysis, IR spectroscopy, single-crystal X-ray diffraction, magnetic measurements and DFT studies. In complex **1** intra-dimer ferromagnetic coupling between Ni^{2+} ions (J = +12.0(2) cm^{-1}) and inter-dimer antiferromagnetic interaction (δ = –0.8(3) cm^{-1}) were observed. DFT-BS calculations provided explanation of ferromagnetic exchange coupling in complex **1**.

[1] Corresponding author: Milica R. Milenković, e-mail: mrm@chem.bg.ac.rs

Key words: Ni(II) complex, Hydrazones, DFT, magnetic properties, crystal structure

1. Introduction

Azide anion is a versatile pseudohalide ligand, which can be coordinated monodentately in mononuclear complexes [1–5] or acts as a bridge between metal centers in di- or polynuclear complexes [6–11]. Azido bridged dinuclear Ni(II) complexes have been studied due to their interesting structural and magnetic properties. Among the reported Ni(II) complexes the most common coordination modes of bridging azido ligands are end-to-end (μ-$_{1,3}$-N_3) and end-on (μ-$_{1,1}$-N_3) (Scheme 1). Bridging azido ligand mediates different types of magnetic exchange interactions, which magnitude depends on the distance between metal ions, dihedral angle between the planes containing metal ions and metal-bridging ligand bond lengths [12]. Antiferromagnetic coupling is associated with end-to-end (μ-$_{1,3}$-N_3) coordination of azido ligand [13–15], while end-on (μ-$_{1,1}$-N_3) coordination mode results in ferromagnetic coupling [16–18], although some exceptions are also reported [19, 20]. Quinoline pharmacophore is present in a large number of natural and synthetic compounds possessing wide range of biological activity [21–24]. Schiff base ligands containing the quinoline moiety and their corresponding metal complexes exhibit significant antitumor and antimicrobial activity [25–32]. Delocalised lipophilic cations (quaternary ammonium and phosphonium salts) can penetrate through the hydrophobic biological membranes and accumulate in cells due to the negative inside transmembrane potential [33]. This property can be used for the formulation of new compounds with enhanced biological activity. Condensation products of Girard's reagents (*N*-substituted glycine hydrazides) with different mono- and dicarbonyl compounds are water soluble quaternary ammonium salts. Such hydrazones can be coordinated in non deprotonated form as cationic ligands or can be deprotonated forming formally neutral zwitter-ions. The presence of additional donor atoms in these ligands allows formation of stable metal chelates and dictates their geometry [34–37]. The azide anion acts as an inhibitor of cytochrome oxidase, mitochondrial F ATP-ase [38] and antioxidant enzymes catalase [39], peroxidase [40] and superoxide dismutase [41]. Azido complexes with Schiff base ligands show considerable biological activity [42–44]. Here, we present synthesis, structural characterization and magnetic properties of dinuclear double end-on azide bridged Ni(II) complex (**1**) $[Ni_2\mathbf{L}_2(\mu\text{-}_{1,1}\text{-}N_3)_2(N_3)_2]$ with the condensation product of 2-quinolinecarboxaldehyde and trimethylammonium

acetohydrazide chloride (Girard's T reagent) (**HL**Cl). Experimental results are confirmed and explained by DFT calculations.

<Scheme 1>

2. Experimental

2.1. Materials and methods

2-Quinolinecarboxaldehyde (97%) and Girard's T reagent (99%) were obtained from Aldrich. IR spectra were recorded on a Nicolet 6700 FT-IR spectrometer using the ATR technique in the region 4000−400 cm^{-1} (s-strong, m-medium, w-weak). ^{1}H (500 MHz), ^{13}C (125 MHz), and 2-D NMR spectra of ligand **HL**Cl were recorded on a Bruker Avance 500 spectrometer at room temperature in methanol−d^4 using TMS as internal standard. Chemical shifts are expressed in ppm (δ) values and coupling constants (*J*) in Hz. Elemental analyses (C, H, and N) were performed by standard micro-methods using the ELEMENTARVario ELIII C.H.N.S.O analyzer. The temperature dependence of magnetic susceptibility was measured on the powder sample using a Quantum Design MPMS-XL-5 SQUID magnetometer, from 2 K to 300 K, and in a 1000 Oe magnetic field. The data were corrected for the contributions of the sample holder and for the diamagnetism of the sample estimated from Pascal's constants.

2.2. Synthesis

*2.2.1. Synthesis of (E)-N,N,N-trimethyl-2-oxo-2-(2-(quinolin-2-ylmethylene)hydrazinyl)ethan-1-aminium chloride (**HL**Cl)*

2-Quinolinecarboxaldehyde 0.31 g (2.00 mmol) was dissolved in ethanol (25 mL) and Girard's T reagent 0.34 g (2.00 mmol) was added. The mixture was refluxed for 3 h. After cooling to the room temperature, a white precipitate was filtered and washed with ethanol. M.p. 210 ^{o}C. Yield: 0.39 g (63%). Elemental analysis calcd for $C_{15}H_{19}ClN_4O$: C 58.73 %, H 6.24 %, N 18.26 %, found: C 58.96 %, H 6.13 %, N 18.02 %. IR (cm^{-1}): 3414 (m), 3062 (m), 2970 (m), 2939 (m), 2831 (m), 1699 (s), 1595 (m), 1562 (w), 1497 (m), 1414 (m), 1379 (w), 1340 (w), 1301 (m),

1230 (m), 1135 (m), 989 (w), 950 (w), 916 (w), 868 (w), 832 (w), 758 (m), 656 (w), 633 (w), 533 (w).

^{1}H NMR (500 MHz, CD_3OD), (numbering of atoms according to Scheme 2a), δ (ppm) 3.47 (s, 9H, C12-H), 4.94 (s, 2H, C11-H), 8.17 (s, 1H, C9-H), 8.18 (d, 1H, $^{3}J_{C3\text{-}H/C4\text{-}H}$ = 10 Hz, C3-H), 8.36 (d, 1H, $^{3}J_{C3\text{-}H/C4\text{-}H}$ = 10 Hz, C4-H), 7.94 (d, 1H, $^{3}J_{C5\text{-}H/C6\text{-}H}$ = 5 Hz C5-H), 7.62 (t, 1H, $^{3}J_{C5\text{-}H/C6\text{-}H/C7\text{-}H}$ =5 Hz, C6-H), 7.78 (t, 1H, $^{3}J_{C6\text{-}H/C7\text{-}H/C8\text{-}H}$ =5 Hz, C7-H), 8.03 (d, 1H, $^{3}J_{C7\text{-}H/C8\text{-}H}$ = 5 Hz, C8-H).

^{13}C NMR (125 MHz, CD_3OD), (numbering of atoms according to Scheme 2a), δ (ppm) 55.0 (C12), 64.4 (C11), 146.9 (C9), 154.4 (C2), 119.2 (C3), 138.7 (C4), 130.1 (C4a), 129.3 (C5), 129.0 (C6), 131.7 (C7), 129.7 (C8), 148.9 (C8a), 167.0 (C10).

*2.2.2. Synthesis of Ni(II) complex (**1**)*

Into the mixture of 0.09 g (0.30 mmol) $Ni(BF_4)_2{\cdot}6H_2O$ and 0.10 g (0.30 mmol) of the ligand **HL**Cl in methanol (20 mL) 0.08 g (1.20 mmol), of NaN_3 was added. The solution was refluxed for 4 h. After refrigeration of reaction solution at –8 °C for two weeks, the red crystals suitable for X-ray analysis were formed. Yield: 0.08 g (31%). Elemental analysis calcd for $C_{31}H_{42}N_{20}Ni_2O_4$: C 42.50 %, H 4.83 %, N 31.97 %, found: C 42.27 %, H 4.68 %, N 31.68 %. IR (cm^{-1}): 3578 (w), 3518 (w), 3342 (w), 3034 (w), 2956 (w), 2823 (w), 2059 (s), 2030 (s), 1644 (w), 1591 (w), 1556 (w), 1530 (m), 1479 (w), 1433 (w), 1400 (w), 1362 (w), 1334 (w), 1301 (m), 1200 (w), 1118 (w), 1086 (m), 1024 (w), 974 (w), 913 (w), 829 (w), 808 (w), 785 (w), 757 (w).

2.3. X-ray structure determinations

Crystal data and refinement parameters of **1** are listed in Table 1. The X-ray intensity data were collected at room temperature with an Agilent SuperNova dual source diffractometer using an Atlas detector and equipped with mirror-monochromated Cu Kα radiation (λ = 1.54184 Å). The data were processed using CRYSALIS PRO [45]. The structure was solved by direct methods implemented in SHELXS–2013 [46] and refined by a full-matrix least-squares procedure based on F^2 using SHELXL-2016 [46]. All non-hydrogen atoms were refined anisotropically. The C9A– and C9B–bound hydrogens and water hydrogen atoms were located in a difference map

and refined with the using distance restraints (DFIX) of C–H or O–H = 0.98 and with U_{iso}(H) = 1.2U_{eq}(C) or U_{iso}(H) = 1.5U_{eq}(O), respectively. All other hydrogen atoms were included in the model at geometrically calculated positions and refined using a riding model.

<Table 1>

2.4. Computational details

Within the present study the density functional theory (DFT) was employed for quantum-chemical modelling of the compounds. For geometry optimizations hybrid exchange-correlation functional B3LYP [47] with Becke's exchange component [48] and the Lee–Yang–Parr correlation functional [49] was used in combination with Pople's group split-valence 6-311G(d,p) basis set extended with polarization functions on non-hydrogen atoms. Molecular model exactly matching ligand **HL**Cl and coordination compound **1** were used. Geometry optimizations were done without any symmetry constrains. The energy minima for all optimized structures were verified by vibration frequency calculations and no vibrations with imaginary frequency were found. Program package Gaussian'03 was employed for calculations [50]. Exchange interaction parameter was evaluated within broken symmetry approximation (DFT-BS) by Ginsberg, Noodleman, Yamaguchi and others [51–53].

We employed three formulas that were proposed and widely used to extract exchange parameter *J* value from the energies of high-spin (HS) and broken symmetry (BS) states, namely spin-projected formula (1) by Noodleman [52], theoretically justified for the case of strong localization of the magnetically active molecular spin-orbitals (SOMOs), non-spin projected formula (2) of Ruiz and others [54, 55], justified for delocalized SOMOs and Yamaguchi formula (3) [53] which is considered to be a "compromise" one between first two. For the case of two interacting spin-centers with equal local spins *S* these formulas are written as follows:

$$J = \frac{(E_{BS} - E_{HS})}{4S^2} \quad (1)$$

$$J = \frac{E_{BS} - E_{HS}}{4S^2 + 2S} \quad (2)$$

$$J = \frac{(E_{BS} - E_{HS})}{\langle S_{HS}^2 \rangle - \langle S_{BS}^2 \rangle} \quad (3)$$

Where E_{BS}, E_{HS},. $\langle S_{BS}^2 \rangle$, $\langle S_{HS}^2 \rangle$ - energies of the broken symmetry (BS), high spin (HS) states, expectation values of spin squared for BS and HS states, correspondingly.

Accuracy of DFT-BS approximation is known to be strongly dependent on the DFT functional used, thus it seems important to employ several functionals to calculate *J* values for comparison purposes and in the order to test the stability of the obtained results. Accounting of the exact Hartree-Fock exchange is well understood to be vital to obtain meaningful quantitative results with DFT-BS [56–58], so for calculations we chose series of hybrid exchange-correlation functionals: B3LYP, modified B3LYP*[59] (differing from the original by reducing exchange HF admixture from 20% to 15%), TPSSh [60] and PBE0 [61]).

For each functional geometry optimizations were performed separately for both HS and BS spin-states without any constrains.

3. Results and discussion

3.1. Synthesis

The ligand (**HL**Cl), *(E)-N,N,N*-trimethyl-2-oxo-2-(2-(quinolin-2-ylmethylene)hydrazinyl)ethan-1-aminium chloride, was obtained in the condensation reaction of 2-quinolinecarboxaldehyde and Girard's T reagent (Scheme 2a). In the reaction of the ligand **HL**Cl with $Ni(BF_4)_2 \cdot 6H_2O$ and NaN_3 in molar ratio 1 : 1 : 4 in methanol dinuclear double end-on azido bridged Ni(II) complex (**1**), with composition $[Ni_2\mathbf{L}_2(\mu\text{-}_{1,1}\text{-}N_3)_2(N_3)_2]$, was obtained (Scheme 2b).

<Scheme 2>

3.2. Spectroscopy

From the IR spectrum of complex **1** it can be seen that the ligand is coordinated in deprotonated form since the new band at 1530 cm^{-1} corresponding to ν($^{-}$O–C=N) vibration of deprotonated hydrazine moiety appeared instead of the band of carbonyl group in the free ligand **HL**Cl at 1699 cm^{-1}. Coordination of the azomethine nitrogen results in red shift of ν(C=N) group, from 1595 cm^{-1} in the spectrum of **HL**Cl ligand to 1591 cm^{-1} in the spectrum of complex **1**. In the IR spectrum of complex **1** two strong bands appeared at 2060 cm^{-1} and 2030 cm^{-1} which can be attributed to the ν_{asym} stretch of the terminal and end-on azido ligands, respectively [62].

2.3. Description of crystal structure

The structure of **1** with atom numbering is shown in Figure 1. The selected bond distances and angles of **1** are listed in Table 2. Complex **1** with formula $[Ni_2\mathbf{L}_2(\mu\text{-}_{1,1}\text{-}N_3)_2(N_3)_2]$ crystallizes in the monoclinic system with space group $P2_1/c$ together with one water and one methanol molecule. The X-ray structure of **1** reveals a neutral dimeric unit where two Ni(II) atoms are bridged by two azido ligands in an end-on mode and with the Ni···Ni separation of 3.281 Å. Each Ni(II) atom is octahedrally coordinated by two N atoms and one O atom from one tridentate ligand **L**, one N atom from one terminal azido ligand and two N atoms from two azido bridging ligands. The terminal azido ligands are coordinated *trans* to each other. The Ni–N bond lengths are in the range from 1.9948 to 2.1850 Å, in which the bond lengths to the quinoline nitrogen atoms N1A and N1B are the longest. Both of the Ni–O distances (2.0997 Å and 2.1373 Å, respectively) are comparable to the corresponding values observed for the Ni–O bond length in similar complexes [3]. All of the Ni–N (bridging azido) bonds in the molecule range from 2.0819 to 2.1400 Å, which are close to the values reported in the other end-on azido Ni(II) complexes [3, 63, 64].

Quinoline fragments are involved in intra- and intermolecular π···π interactions and intermolecular interactions of C–H···π(quinoline ring) type. The π···π interactions between quinoline rings comprise arene-arene, arene-pyridine and pyridine-pyridine contacts. Solvent

water molecule serving as double hydrogen bond donor (toward N6Z and N3B at *x*, 3/2–*y*, –1/2+*z*) mediate in joining the dimeric units into infinite chains running parallel to *c* direction. The neighboring infinite chains are linked through intermolecular π···π interactions of pyridine-pyridine and arene-pyridine type and C–H···π(quinoline ring) interactions. Geometric parameters describing π···π, C–H···π(ring) and hydrogen bonding interactions are given in the Supplementary material together with graphical presentation of crystal packing.

<Fig. 1>

<Table 2>

3.4. Magnetic measurements

Magnetic data are shown in Figure 2, where temperature dependence of χT and inverse magnetic susceptibility ($1/\chi$) per mol of Ni(II) are presented. It can be seen that there is a linear behavior of inverse magnetic susceptibility for the temperature above 150 K. Fitting the susceptibility data for $T > 150$ K to the Curie–Weiss law $\chi = C/(T - \theta)$ (where C and θ present Curie constant and Weiss temperature, respectively), gave C = 1.25 $cm^3mol^{-1}K^{-1}$, and θ = +24.0 K. The effective magnetic moment μ_{eff} = 3.16 μ_B, obtained from Curie constant C, is slightly higher than the spin-only value for Ni^{2+} ion (μ_{eff} = 2.82 μ_B), but it is in a good agreement with literature data for Ni^{2+} in octahedral environment [65, 66]. Positive values of Weiss constant speak in favor of strong ferromagnetic coupling between two Ni^{2+} ions. It can be seen that upon cooling χT value increases and shows broad maximum around 23 K (1.89 emu K/mol) indicating the presence of dominant ferromagnetic interaction. Upon further cooling this product decreases sharply to 1.28 emu K/mol at 2 K. This decrease may be due to the intermolecular antiferromagnetic exchange interactions.

In order to evaluate the exchange coupling constants, Eq. (4) was employed [67]:

$$\chi_M = \frac{Ng^2\mu_B^2}{k_B(T-\delta)}\left(\frac{\exp(2J/k_BT)+5\exp(6J/k_BT)}{1+3\exp(2J/k_BT)+5\exp(6J/k_BT)}\right)+N\alpha. \quad (4)$$

In this equation J is exchange integral between two Ni^{2+} spins (S = 1), $N\alpha$ is temperature independent paramagnetism and δ is an effective Weiss constant included in equation to take account of inter-dimmer interaction. Least-squares fitting of all experimental data (Figure 2) leads to the following parameters J = +12.0(2) cm^{-1}, g = 2.3(1), δ = -0.8(3) cm^{-1} and $N\alpha$ = $382\cdot10^{-6}$ emu/mol. R value defined as $R=\sum[\chi_{obs}-\chi_{calc}]^2/\sum[\chi_{obs}]^2$ was found to be $3.2\cdot10^{-6}$. Positive J value confirms significant intra-dimer ferromagnetic coupling. The negative δ value shows inter-dimer antiferromagnetic interactions which causes sharp decrease of χT below 20 K.

<Fig. 2>

It has been shown in the literature, that dinuclear complexes with the azido bridges, exhibit different magnetic behavior, depending upon several parameters like bridging modality, the bridge angles and dimensions of the nuclear centers. The most important is bridging modality which can be two-fold: end-to-end (μ-$_{1,3}$-N_3) or end-on (μ-$_{1,1}$-N_3) (see Scheme 1). As a general rule, the first modality shows, almost exclusively, antiferromagnetic interaction between metallic cations [13–15], while for the later one is characteristic ferromagnetic exchange coupling [16–18]. In investigated complex, end-on coordination mode of the bridging ligands was found (Section 3.3) and thus, obtained ferromagnetic interaction is in accordance with the mentioned rule. Found structural parameters (Section 3.3), like the bridging M–N–M angle (102°), the M–N bond distance (2.1 Å) and Ni···Ni separation (3.281 Å), are also very important and affect the strength of the exchange interaction [68]. Determined J value for complex **1** is comparable with the literature data relating to the similar dinuclear nickel compounds with two μ-$_{1,1}$-azide bridges. For example, complexes $[Ni_2(L^1)(HL^1)(\mu\text{-}_{1,1}\text{-}N_3)_2]ClO_4$ (HL^1 = *N*,*N*-bis(2-methylpyridyl)-3,5-dimethyl-2-hydroxybenzylamine) with Ni···Ni 3.240 Å, N–Ni–N ~ 98°, J = 12.26 cm^{-1}, δ = -0.42 cm^{-1}, g = 2.31 [69] and $[Ni(terpy)(\mu\text{-}_{1,1}\text{-}N_3)(N_3)]_2\cdot2H_2O$ with Ni···Ni 3.276 Å, N–Ni–N 101.3°, J = 20.1 cm^{-1} [70].

3.5. Comparison of structural and magnetic parameters of bis(μ-$_{1,1}$-azido)nickel(II) complexes

The structural parameters correlating the geometry of related ferromagnetically coupled bis(μ-$_{1,1}$-azido)nickel(II) complexes [16, 62–64, 71–78] are listed in Table 3. In the analyzed dinuclear Ni(II) complexes of octahedral geometry N_3^- anions act both as end-on bridging and as terminal ligands. The chelating ligands are tridentate in all cases except in $[Ni_2(L^2)(N_3)_4]$ [71] and $[Ni(L^{14})(N_3)_4]$ [77] complexes in which ligands L^2 and L^{14} act as bis-tridentate. The complexes presented in Table 3 differ in position of $N_{azido(terminal)}$ atoms with respect to the $Ni_2N_{2(azido(end\text{-}on))}$ plane, as evidenced by the $N_{azido(terminal)}$–Ni–$N_{azido(end\text{-}on)}$–Ni torsion angles. The analysis of Ruiz *et al*. performed on bis(μ-azido)nickel(II) complexes has predicted ferromagnetic interaction on all ranges of Ni–N(N_3)–Ni angles, with *J* increasing upon increasing this angle, yielding a maximum at 104° approximately [78]. They have also shown that the bond distance between the metal and bridging atoms has a strong influence on the coupling constant, with the ferromagnetic coupling diminishing upon increasing such distance. The smallest Ni–$N_{azido(end\text{-}on)}$–Ni angles of ≈ 98° were found in complexes **2** and **12** and in one moiety of complex **4** which lies at special position in the unit cell. The largest Ni–$N_{azido(end\text{-}on)}$–Ni bond angle of 103.9° is found in complex **7**. For the most complexes considered here the Ni–$N_{azido(end\text{-}on)}$–Ni bond angles within the same $Ni_2N_{2(azido(end\text{-}on))}$ rhombus are comparable in magnitude, however, the significant difference of +3° has been observed in complex **5**. The Ni···Ni separation is relatively large and range from 3.155 to 3.448 Å (Table 3). The $[Ni_2(L^2)(N_3)_4]$ complex has the slightly shorter Ni···Ni separation compared with the other complexes listed in Table 3. This may be attributed to the structure of ligand L^2 and its bis-tridentate coordination function.

<Table 3>

3.6. Theoretical calculations

Possible isomers of **HL**Cl ligand are geometric isomers (*E* and *Z*) related to the azomethine group, keto and enol tautomers (hydrazone and α-oxyazine) and rotational isomers (*syn* and *anti*). Quantum-chemical calculations of the geometry and total energy of possible isomeric

forms of **HL**Cl were performed to give insight into their stability. The results are shown in Figure 3.

<Fig. 3>

Both in the gas phase and in methanol solution rotamers of hydrazonic tautomer of **HL**Cl (structures **a**–**c**) are much more stabilized than α-oxyazine ones (structures **d**, **e**), more than by 14 kcal/mol. In vacuum the global minimum corresponds to hydrazonic isomer **a**, stabilized by intramolecular NH···N hydrogen bond between hydrazine fragment and cyclic quinoline nitrogen atom, isomer **b** is destabilized by 5.9 kcal/mol. But when methanol media is taken into account, the most stable appeared to be rotamer **b**, which has energy 1.6 kcal/mol lower, than that of rotamer **a**. Isomer **c** is strongly destabilized both in vacuum and methanol solution. These results were confirmed from the ^{1}H NMR spectrum of **HL**Cl in methanol in which two sets of signals of both **a** and **b** isomers were observed with molar ratio 1 : 4, respectively.

Exchange interactions in binuclear complex **1** were modeled within broken symmetry approach (DFT-BS). In Table 4 *J* values calculated with formulas (1)–(3) (see Experimental section) and various hybrid exchange-correlation functionals are given (calculated energies of HS and BS states and other calculation details can be found in Table S.4 of Supplementary material).

<Table 4>

The ferromagnetic type of exchange interaction in the complex **1** is predicted in all considered cases. It is seen that while Yamaguchi and spin-projected formulas give virtually the same values and noticeably overestimate the exchange coupling strength, values obtained with Ruiz formula are in reasonably good agreement with the experimental value. Though all DFT functionals give close results (within the 9 cm^{-1} range), the closest to experimental *J* value is obtained with modified B3LYP* functional. Good results with this functional for calculating energies of spin

states were reported recently [79, 80]. Further the results obtained with this functional will be reported, the values for the other ones are given in the Supplementary material. Ni(II) ion with d^8 electronic configuration in octahedral environment is characterized with local spin $S = 1$. Shapes of the four localized magnetically active single occupied molecular orbitals (SOMOs) are shown in Figure 4. For each metal center there are two SOMOs, with predominant input of $d_{x^2-y^2}$–like AO (in local coordinate system) lying in the basal plane defined by four nitrogen donor atoms (see Figure 4, left) and d_{z^2}-like AO, oriented along the axial line defined by quinoline nitrogen donor atom and carbonyl oxygen (Figure 4, right).

<Fig. 4>

First two orbitals are more delocalized towards ligands, including bridging azide nitrogens, while latter two are localized on *d*-AO and axial donors, this difference is illustrated by overlap integral value –0.0305 for first pair and only 0.0067 for latter. Small overlap of SOMOs results in more pronounced partition of α and β-spin electronic density (SD) in broken symmetry state, and is the reason for ferromagnetic type interaction between paramagnetic centers (see Figure 5 and Table 5 for SD distribution and Mulliken charges/spin populations in complex **1**).

<Fig. 5>

It is clearly seen that SD density is strongly localized on the metal centers with only minor delocalization over the nearest donor atoms of the organic ligand, more than 1.6e out of total 2e spin density is localized on Ni centers. On the nitrogen atoms of the bridging N_3^- anions SD is very small, even in triplet state –0.025 and 0.015e on nitrogen atoms N1Z and N4Z, correspondingly (see Table 5).

<Table 5>

Switching between high and low spin-states have minor influence on charge distribution, leading only to inversion of the spin population sign on one of the two Ni centers and decrease of the spin population on the bridging atoms due to partial α- and β-SD overlap.

4. Conclusion

Complex **1** was obtained in the reaction of the condensation product of 2-quinolinecarboxaldehyde and Girard's T reagent with $Ni(BF_4)_2 \cdot 6H_2O$ and NaN_3. In complex **1** octahedral surrounding around each of the two Ni(II) centers consist of NNO coordinated deprotonated hydrazone ligand, one monodentate azido ligand and two azido bridging ligands. Magnetic data for complex **1** showed very intensive intra-dimer ferromagnetic coupling between Ni^{2+} ions and inter-dimer antiferromagnetic interaction. DFT-BS modeling demonstrated that ferromagnetic exchange coupling in complex **1** is determined by small magnetically active SOMOs of the metal centers overlap and their minor delocalization towards nitrogen atoms of the bridging azide anions.

Appendix A. Supplementary data

CCDC 1524733 contains the supplementary crystallographic data for **1**. These data can be obtained free of charge via http://www.ccdc.cam.ac.uk/conts/retrieving.html, or from the Cambridge Crystallographic Data Centre, 12 Union Road, Cambridge CB2 1EZ, UK; fax: (+44) 1223-336-033; or e-mail: deposit@ccdc.cam.ac.uk.

Acknowledgements

This work was supported by the Ministry of Education, Science and Technological development of the Republic of Serbia (Grant OI 172055), Slovenian Research Agency (P-0175) and internal grant of SFedU No. 213.01-07-2014/03PChVG. We thank the EN-FIST Centre of Excellence,

Ljubljana, Slovenia, for use of the SuperNova diffractometer. DFT calculations were performed on the clusters of the joint resource center "High performance calculation" of Southern Federal University. Part of this work was supported by COST Action CM1305 "Explicit Control Over Spin-states in Technology and Biochemistry (ECOSTBio)".

References

[1] S. Meghdadi, K. Mereiter, M. Amirnasr, F. Karimi, A. Amiri, Polyhedron 68 (2014) 60.

[2] R.A. de Souza, A. Stevanato, O. Treu-Filho, A.V.G. Netto, A.E. Mauro, E.E. Castellano, I.Z. Carlos, F.R. Pavan, C.Q.F. Leite, Eur. J. Med. Chem. 45 (2010) 4863.

[3] B. Shaabani, A.A. Khandar, M. Dusek, M. Pojarova, M.A. Maestro, R. Mukherjee, F. Mahmoudi, J. Coord. Chem. 67 (2014) 2096.

[4] B. Shaabani, A.A. Khandar, F. Mahmoudi, S.S. Balula, L. Cunha-Silva, J. Mol. Struct. 1045 (2013) 55.

[5] S.B. Novaković, G.A. Bogdanović, I.D. Brčeski, V.M. Leovac, Acta Crystallogr. C65 (2009) m263.

[6] F.A. Mautner, C. Berger, M.J. Dartez, Q.L. Nguyen, J. Favreau, S.S. Massoud, Polyhedron 69 (2014) 48.

[7] B. Machura, A. Świtlicka, I. Nawrot, J. Mroziński, K. Michalik, Polyhedron 30 (2011) 2815.

[8] B. Machura, I. Nawrot, K. Michalik, Polyhedron 31 (2012) 548.

[9] J. Cano, F.A. Mautner, C. Berger, R.C. Fischer, R. Vicente, Polyhedron 50 (2013) 240.

[10] M. Das, S. Chatterjee, S. Chattopadhyay, Polyhedron 68 (2014) 205.

[11] S. Banerjee, C. Adhikary, C. Rizzoli, R. Pal, Inorg. Chim. Acta 409 (2014) 202.

[12] J. Ribas, A. Escuer, M. Monfort, R. Vicente, R. Corteś, L. Lezama, T. Rojo, Coord. Chem. Rev. 193–195 (1999) 1027.

[13] S.-Q. Bai, C.-J. Fang, Z. He, E.-Q. Gao, C.-H. Yan, T.S.A. Hora, Dalton Trans. 41 (2012) 13379.

[14] S.S. Massoud, F.A. Mautner, R. Vicente, A.A. Gallo, E. Ducasse, Eur. J. Inorg. Chem. (2007) 1091.

[15] M.-L. Bonnet, C. Aronica, G. Chastanet, G. Pilet, D. Luneau, C. Mathonière, R. Clérac, V. Robert, Inorg. Chem. 47 (2008) 1127.

[16] S.S. Massoud, F.R. Louka, Y.K. Obaid, R. Vicente, J. Ribas, R.C. Fischerc, F.A. Mautner, Dalton Trans. 42 (2013) 3968.

[17] P. Mukherjee, M.G.B. Drew, C.J. Gómez-García, A. Ghosh, Inorg. Chem. 48 (2009) 5848.

[18] S.K. Dey, N. Mondal, M.S.E. Fallah, R. Vicente, A. Escuer, X. Solans, M. Font-Bardía, T. Matsushita, V. Gramlich, S. Mitra, Inorg. Chem. 43 (2004) 2427.

[19] C.S. Hong, J.-E. Koo, S.-K. Son, Y.S. Lee, Y.-S. Kim, Y. Do, Chem. Eur. J. 7 (2001) 4243.

[20] P. Chaudhuri, R. Wagner, S. Khanra, T. Weyhermüller, Dalton Trans. (2006) 4962.

[21] V.R. Solomon, H. Lee, Curr. Med Chem. 18 (2011) 1488.

[22] K. Kaur, M. Jain, R.P. Reddy, R. Jain, Eur. J. Med. Chem. 45 (2010) 3245.

[23] S. Kumar, S. Bawa, H. Gupta, Mini-Rev. Med. Chem. 9 (2009) 1648.

[24] J.P. Michael, Nat. Prod. Rep. 25 (2008) 166.

[25] F. Bisceglie, A. Musiari, S. Pinelli, R. Alinovi, I. Menozzi, E. Polverini, P. Tarasconi, M. Tavone, G. Pelosi, J. Inorg. Biochem. 152 (2015) 10.

[26] S. Adsule, V. Barve, D. Chen, F. Ahmed, Q.P. Dou, S. Padhye, F.H. Sarkar, J. Med. Chem. 49 (2006) 7242.

[27] X. Fan, J. Dong, R. Min, Y. Chen, X. Yi, J. Zhou, S. Zhang, J. Coord. Chem. 66 (2013) 4268.

[28] S. Zhang, J. Dong, X. Fan, Y. Chen, J. Zhou, J. Coord. Chem. 65 (2012) 3098.

[29] N. Filipović, N. Polović, B. Rašković, S. Misirlić-Denčić, M. Dulović, M. Savić, M. Nikšić, D. Mitić, K. Anđelković, T. Todorović, Monatsh. Chem. 145 (2014) 1089.

[30] N. Gligorijević, T. Todorović, S. Radulović, D. Sladić, N. Filipović, D. Gođevac, D. Jeremić, K. Anđelković, Eur. J. Med. Chem. 44 (2009) 1623.

[31] N. Filipović, T. Todorović, R. Marković, A. Marinković, S. Tufegdžić, D. Gođevac, K. Anđelković, Transition Met. Chem. 35 (2010) 765.

[32] N. Filipović, H. Borrmann, T. Todorović, M. Borna, V. Spasojević, D. Sladić, I. Novaković, K. Andjelković, Inorg. Chim. Acta 362 (2009) 1996.

[33] J.S. Modica-Napolitano, J.R. Aprille, Adv. Drug Delivery Rev. 49 (2001) 63.

[34] L.S. Vojinović-Ješić, S.B. Novaković, V.M. Leovac, V.I. Češljević, J. Serb. Chem. Soc. 77 (2012) 1129.

[35] S.J. Azhari, S. Salah, R.S. Farag, M.M. Mostafa, Spectrochim. Acta, Part A 136 (2015) 1903.

[36] B. Čobeljić, A. Pevec, S. Stepanović, V. Spasojević, M. Milenković, I. Turel, M. Swart, M. Gruden-Pavlović, K. Adaila, K. Anđelković, Polyhedron 89 (2015) 271.

[37] G. Brađan, A. Pevec, I. Turel, I.N. Shcherbakov, M. Milenković, M. Milenković, D. Radanović, B. Čobeljić, K. Anđelković, J. Coord. Chem. 69 (2016) 2754.

[38] M.W. Bowler, M.G. Montgomery, A.G.W. Leslie, J.E. Walker, Proc. Natl. Acad. Sci. U. S. A. 103 (2006) 8646.

[39] C. Sanchis-Segura, M. Miquel, M. Correa, C.M.G. Aragon, Alcohol 19 (1999) 37.

[40] P.R.O. de Montellano, S.K. David, M.A. Ator, D. Tew, Biochemistry 27 (1988) 5470.

[41] H.P. Misra, I. Fridovich, Arch. Biochem. Biophys. 189 (1978) 317.

[42] B. Čobeljić, M. Milenković,·A. Pevec, I. Turel, M. Vujčić, B. Janović, N. Gligorijević, D. Sladić, S. Radulović,·K. Jovanović,·K. Anđelković, J. Biol. Inorg. Chem. 21 (2016) 145.

[43] S. Banerjee, S. Mondal, W. Chakraborty, S. Sen, R. Gachhui, R.J. Butcher, A. M. Z. Slawin, C. Mandal, S. Mitra, Polyhedron 28 (2009) 2785.

[44] B. Shaabani, A.A. Khandar, H. Mobaiyen, N. Ramazani, S.S. Balula, L. Cunha-Silva, Polyhedron 80 (2014) 166.

[45] Oxford Diffraction, CrysAlis PRO, Oxford Diffraction Ltd., Yarnton, England, 2009.

[46] G.M. Sheldrick, Acta. Crystallogr. A64 (2008) 112.

[47] A.D. Becke, J. Chem. Phys. 98 (1993) 5648.

[48] A.D. Becke, Phys. Rev. A 38 (1988) 3098.

[49] C. Lee, W. Yang, R.G. Parr, Phys. Rev. B 37 (1988) 785.

[50] M.J. Frisch, G.W. Trucks, H.B. Schlegel, G.E. Scuseria, M.A. Robb, J.R. Cheeseman, J.J. A. Montgomery, T. Vreven, K.N. Kudin, J.C. Burant, J.M. Millam, S.S. Iyengar, J. Tomasi, V. Barone, B. Mennucci, M. Cossi, G. Scalmani, N. Rega, G.A. Petersson, H. Nakatsuji, M. Hada, M. Ehara, K. Toyota, R. Fukuda, J. Hasegawa, M. Ishida, T. Nakajima, Y. Honda, O. Kitao, H. Nakai, M. Klene, X. Li, J.E. Knox, H.P. Hratchian, J.B. Cross, C. Adamo, J. Jaramillo, R. Gomperts, R.E. Stratmann, O. Yazyev, A.J. Austin, R. Cammi, C. Pomelli, J.W. Ochterski, P.Y. Ayala, K. Morokuma, G.A. Voth, P. Salvador, J.J. Dannenberg, V.G. Zakrzewski, S. Dapprich, A.D. Daniels, M.C. Strain, O. Farkas, D.K. Malick, A.D. Rabuck, K. Raghavachari, J.B. Foresman, J.V. Ortiz, Q. Cui, A.G. Baboul, S. Clifford, J. Cioslowski, B.B. Stefanov, G. Liu, A. Liashenko, P. Piskorz, I. Komaromi, R.L. Martin, D.J. Fox, T. Keith, M.A. Al-Laham, C.Y.

Peng, A. Nanayakkara, M. Challacombe, P.M.W. Gill, B. Johnson, W. Chen, M.W. Wong, C. Gonzalez, J.A. Pople, Gaussian 03, revision D.01, Gaussian, Inc., Pittsburg, PA, 2003.

[51] A.P. Ginsberg, J. Am. Chem. Soc. 102 (1980) 111.

[52] L. Noodleman, C.Y. Peng, D.A. Case, J.M. Mouesca, Coord. Chem. Rev. 144 (1995) 199.

[53] K. Yamaguchi, Y. Takahara, T. Fueno, in: J.V.H. Smith, H.F. Schaefer, K. Morokuma (Eds.), Applied Quantum Chemistry, Reidel, Dordrecht, 1986, p. 155.

[54] E. Ruiz, J. Cano, S. Alvarez, P. Alemany, J. Comput. Chem. 20 (1999) 1391.

[55] E. Ruiz, S. Alvarez, J. Cano, V. Polo, J. Chem. Phys. 123 (2005) 164110.

[56] P. Comba, S. Hausberg, B. Martin, J. Phys. Chem. A 113 (2009) 6751.

[57] I. Ciofini, C.A. Daul, Coord. Chem. Rev. 238–239 (2003) 187.

[58] N.A.G. Bandeira, B. Le Guennic, J. Phys. Chem. A 116 (2012) 3465.

[59] M. Reiher, O. Salomon, A. Hess, Theor. Chem. Acc. 107 (2001) 48.

[60] V.N. Staroverov, G.E. Scuseria, J. Tao, J.P. Perdew, J. Chem. Phys. 119 (2003) 12129.

[61] C. Adamo, V. Barone, J. Chem. Phys. 110 (1999) 6158.

[62] M.G. Barandika, R. Cortés, L. Lezama, M.K. Urtiaga, M.I. Arriortua, T. Rojo, J. Chem. Soc., Dalton Trans. (1999) 2971.

[63] H.-D. Bian, W. Gu, Q. Yu, S.-P. Yan, D.-Z. Liao, Z.-H. Jiang, P. Cheng, Polyhedron 24 (2005) 2002.

[64] A. Solanki, M. Monfort, S.B. Kumar, J. Mol. Struct. 1050 (2013) 197.

[65] B. Čobeljić, B. Warżajtis, U. Rychlewska, D. Radanović, V. Spasojević, D. Sladić, R. Eshkourfu, K. Anđelković, J. Coord. Chem. 65 (2012) 655.

[66] S. Wöhlert, T. Runčevski, R.E. Dinnebier, S.G. Ebbinghaus, C. Näther, Cryst. Growth Des. 14 (2014) 1902.

[67] A.P. Ginsberg, R.C. Sherwood, R.W. Brookes, R.L. Martin, J. Am. Chem. Soc. 93 (1971) 5927.

[68] L.K. Thompson, S.S. Tandon, Comments Inorg. Chem. 18 (1996) 125.

[69] S. Sarkar, A. Mondal, A. Banerjee, D. Chopra, J. Ribas, K.K. Rajak, Polyhedron 25 (2006) 2284.

[70] M.I. Arriortua, A.R. Cortes, L. Lezama, K.T. Rojo, X. Solans, M. Font-Bardia, Inorg. Chim. Acta 174 (1990) 263.

[71] S. Deoghoria, S. Sain, M. Soler, W.T. Wong, G. Christou, S.K. Bera, S.K. Chandra, Polyhedron 22 (2003) 257.

[72] S. Sarkar, A. Mondal, M.S.E. Fallah, J. Ribas, D. Chopra, H. Stoeckli-Evans, K.K. Rajak, Polyhedron 25 (2006) 25.

[73] S. Liang, Z. Liu, N. Liu, C. Liu, X. Di, J. Zhang, J. Coord. Chem. 63 (2010) 3441.

[74] R. Cortés, J.I. Ruiz de Larramendi, L. Lezama, T. Rojo, K. Urtiaga, M.I. Arriortua, J. Chem. Soc. Dalton Trans. (1992) 2723.

[75] A. Escuer, R. Vicente, J. Ribas, X. Solans, Inorg. Chem. 34 (1995) 1793.

[76] S. Nandi, D. Bannerjee, J.-S. Wu, T.-H. Lu, A.M.Z. Slawin, J.D. Woollins, J. Ribas, C. Sinha, Eur. J. Inorg. Chem. (2009) 3972.

[77] S. Sain, S. Bid, A. Usman, H.-K. Fun, G. Aromíc, X. Solans, S.K. Chandra, Inorg. Chim. Acta 358 (2005) 3362.

[78] E. Ruiz, J. Cano, S. Alvarez, P. Alemany, J. Am. Chem. Soc., 120 (1998) 11122.

[79] M. Reiher, Inorg. Chem. 41 (2002) 6928.

[80] V.I. Minkin, A.A. Starikova, A.G. Starikov, Dalton Trans. 45 (2016) 12103.

Scheme captions

Scheme 1. The most common coordination modes of bridging azido ligands to Ni(II) (end-to-end (μ-$_{1,3}$-N_3) and end-on (μ-$_{1,1}$-N_3)).

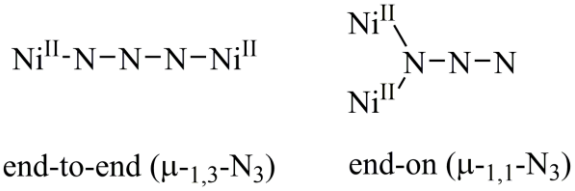

Scheme 2. Synthesis of ligand **HL**Cl and complex **1**

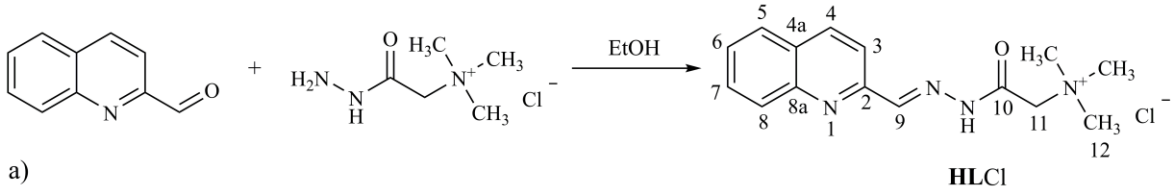

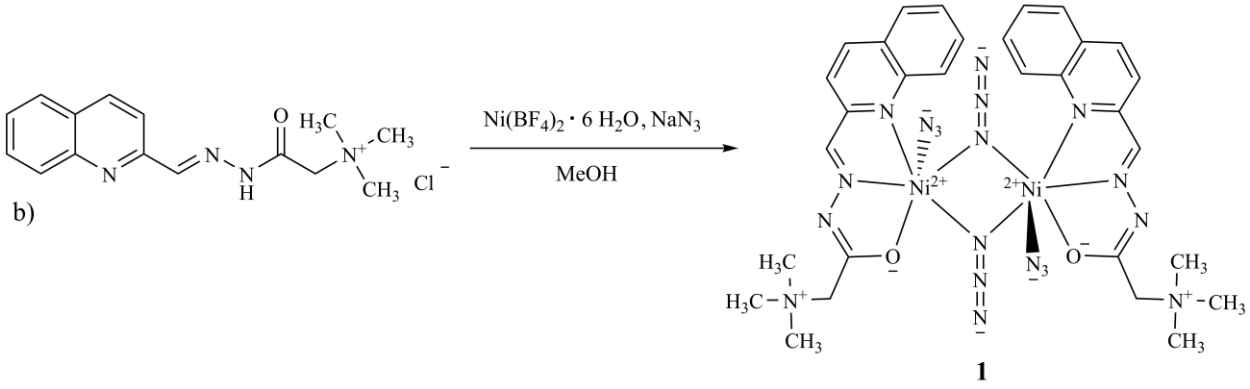

Figure captions

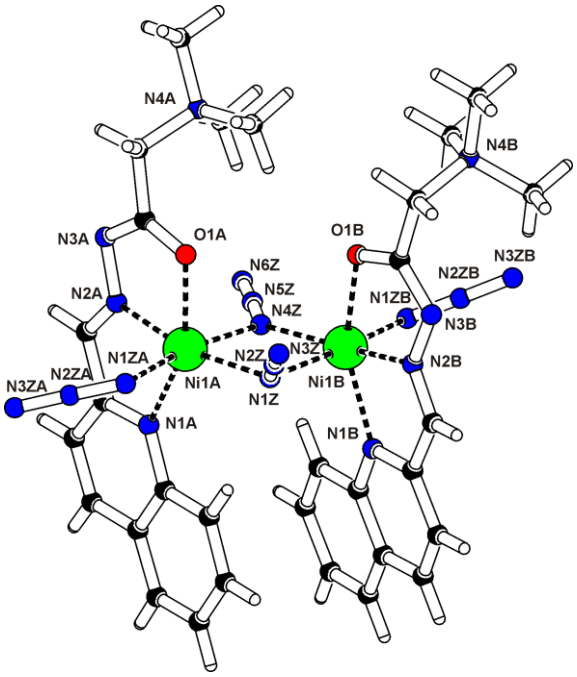

Figure 1. Graphical representation of **1**. Non-coordinated water and methanol molecules have been left out for clarity.

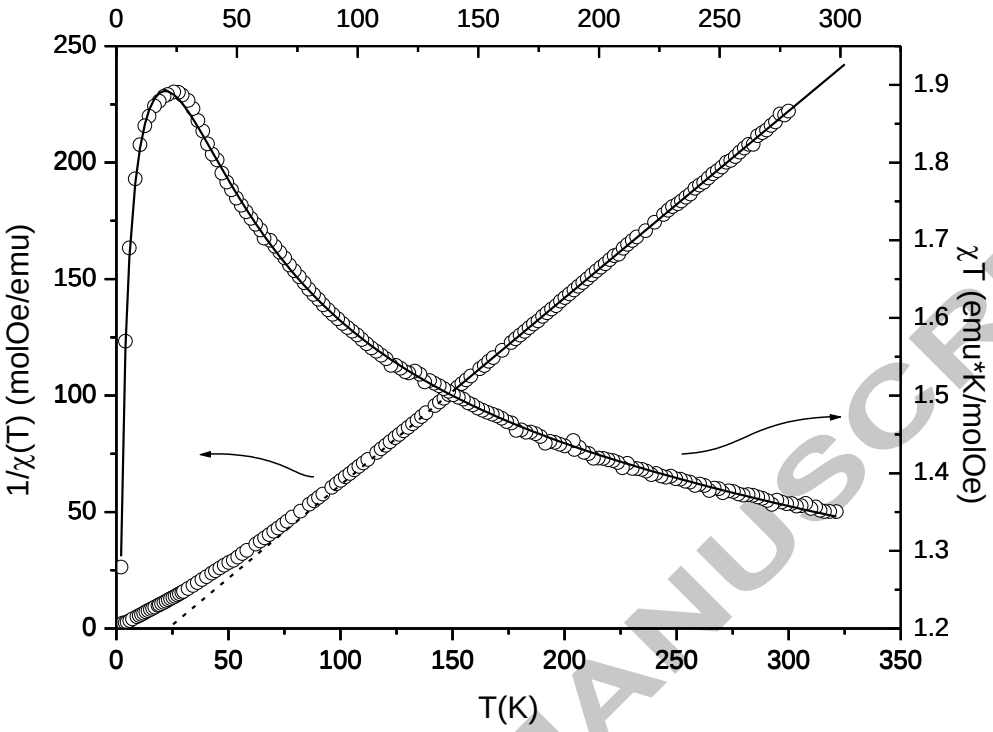

Figure 2. Temperature dependences of χT and inverse susceptibility. Solid line is the best fit of the experimental data using eq. 4 and Curie-Weiss law.

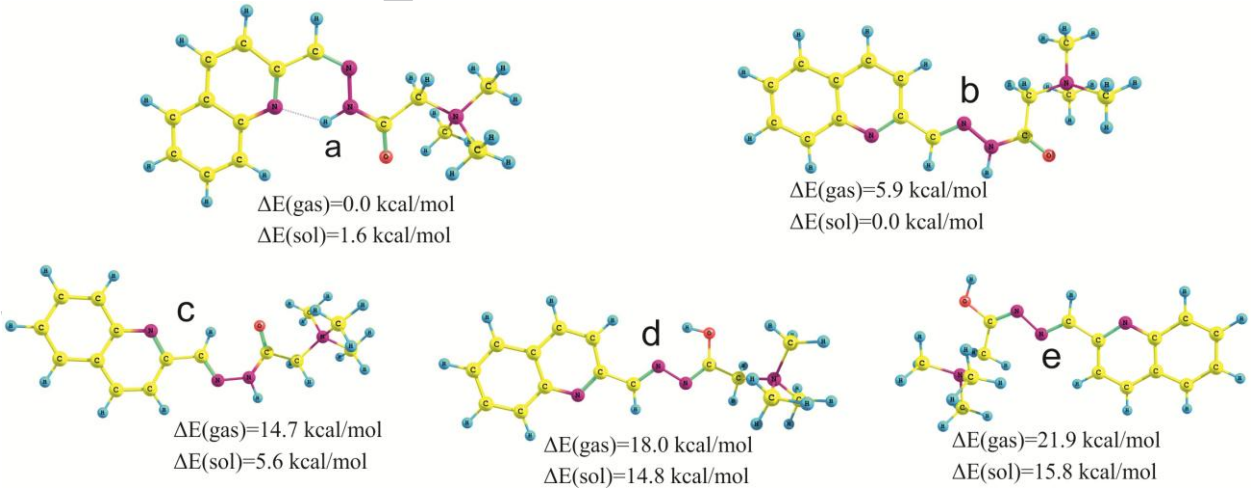

Figure 3. Relative stability ΔE (kcal mol^{-1}) of **HL**Cl isomers in vacuum and methanol.

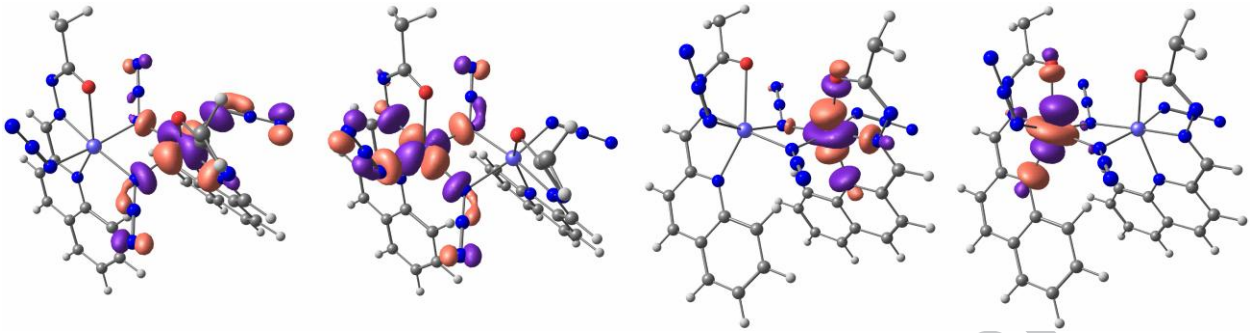

Figure 4. Shape of the localized magnetically active SOMOs of the complex **1** (grey spheres – carbon, blue – nitrogen, red – oxygen atoms, cyan – nickel; trimethylammonium group is removed for clarity, contour value is 0.04 e·Å^{-3}).

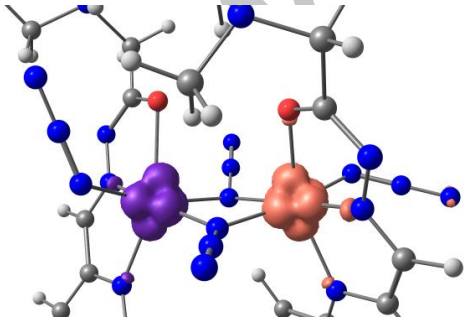

Figure 5. SD in the BS state of complex **1** (pink and magenta surfaces – α and β spin, contour value 0.02 e·Å^{-3})

Table captions

Table 1. Crystal data and structure refinement details for **1**.

	1
formula	$C_{31}H_{42}N_{20}Ni_2O_4$
Fw (g mol^{-1})	876.26
crystal size (mm)	0.25 x 0.20 x 0.10
crystal color	Red
radiation, wavelength (Å)	CuKα, 1.54184
crystal system	Monoclinic
space group	$P2_1/c$
a (Å)	15.6460(3)
b (Å)	11.9586(2)
c (Å)	22.3571(5)
β (º)	107.206(2)
V (Å^3)	3995.90(14)
Z	4
calcd density (g cm^{-3})	1.457
F(000)	1824
no. of collected reflns	15303
no. of independent reflns	7812
R_{int}	0.0206
no. of reflns observed	6375
no. parameters	540
$R[I > 2\sigma(I)]^a$	0.0389
wR_2 (all data)^b	0.1128
Goof , S^c	1.037
maximum/minimum residual electron density (e Å^{-3})	+0.384/–0.346

^{a} $R = \sum||F_o| - |F_c||/\sum|F_o|$. ^{b} $wR_2 = \{\sum[w(F_o^2 - F_c^2)^2]/\sum[w(F_o^2)^2]\}^{1/2}$.

[c] $S = \{\sum[w(F_o^2 - F_c^2)^2]/(n-p)\}^{1/2}$ where n is the number of reflections and p is the total number of parameters refined

Table 2. Selected bond lengths (Å) and angles (°) for **1**.

Ni1A–N1A	2.1850(18)	O1A–Ni1A–N1A	153.82(6)
Ni1A–N2A	1.9948(17)	O1A–Ni1A–N2A	76.80(7)
Ni1A–N1Z	2.0851(17)	O1A–Ni1A–N1Z	93.35(7)
Ni1A–N4Z	2.1400(19)	O1A–Ni1A–N4Z	92.17(7)
Ni1A–N1ZA	2.063(2)	O1A–Ni1A–N1ZA	91.58(8)
Ni1A–O1A	2.0997(15)	O1B–Ni1B–N1B	152.96(7)
Ni1B–N1B	2.1793(19)	O1B–Ni1B–N2B	75.77(7)
Ni1B–N2B	1.9962(18)	O1B–Ni1B–N1Z	93.13(7)
Ni1B–N1Z	2.1339(18)	O1B–Ni1B–N4Z	97.35(7)
Ni1B–N4Z	2.0819(18)	O1B–Ni1B–N1ZB	90.37(8)
Ni1B–N1ZB	2.064(2)	Ni1A–N1Z–Ni1B	102.11(7)
Ni1B–O1B	2.1373(16)	Ni1A–N4Z–Ni1B	102.01(8)

Table 3. Structural and magnetic parameters of related bis(μ-$_{1,1}$-azido) bridged Ni(II) complexes

Complex		Ni–$N_{azido(end-on)}$–Ni (°) (mean value)	Ni···Ni (Å)	Ni–$N_{azido(end-on)}$ (Å)	$N_{azido(terminal)}$–Ni–$N_{azido(end-on)}$–Ni (°)	J (cm^{-1})	Ref.
$[Ni_2L_2(N_3)_4]\cdot H_2O\cdot CH_3OH$	(**1**)	102.11(7), 102.01(8) (102.06)	3.281	2.085(2), 2.140(2)	-21.4(5), -179.82(9), -179.07(9), -19.6(6)	+12.0(2)	This work
$[Ni_2(L^2)(N_3)_4]^a$	(**2**)	98.36(8), 97.66(9) (98.01)	3.155	2.061(2), 2.061(2), 2.108(2), 2.130(2)	3.5(7), 159.1(1), 10.0(7), 160.0(1)	+21.8	[71]
$[Ni_2(L^3)_2(N_3)_4]^b$	(**3**)	99.7(4)	3.191(4)	2.086(8), 2.088(9)	93.4(3), -89.7(3)	+34.2	[72]
$[Ni_2(L^4)_2(N_3)_4]^c$	(**4**)	101.3(1), 100.0(1) (100.65), 97.6(1)	3.296, 3.221	2.085(2), 2.117(2), 2.184(2), 2.176(2), 2.180(2), 2.101(2)	102.9(1), -100.8(1), -82.6(1), 78.9(1), 87.6(1), -89.8(1)	+22.7	[72]
$[Ni_2(L^5)_2(N_3)_4]\cdot CH_3OH^d$	(**5**)	103.3, 100.3 (101.79)	3.395, 3.333	2.155(3), 2.142(3), 2.174(3), 2.200(3)	96.3(2), -92.9(2), 92.7(1), -91.4(1)	+1.91	[63]
$[Ni_2(L^6)_2(N_3)_4]\cdot H_2O^e$	(**6**)	98.7(2), 98.5(2) (98.6)	3.190(1)	2.075(4), 2.080(4), 2.132(4), 2.131(4)	21.0(2), 165.9(2), 161.2(2), -9.5(9)	+28.32	[73]
$[Ni(L^7)_2(N_3)_4]\cdot 1.5H_2O^f$	(**7**)	103.9(1)	3.3522(7)	2.138(3), 2.120(3)	-83.8(1), 90.7(1)	+51.0(2)	[16]
$[Ni(L^8)_2(N_3)_4]^g$	(**8**)	102.2(2), 101.0(2) (101.6)	3.297(1)	2.109(5), 2.163(6), 2.128(6), 2.107(5)	20.0(2), -177.0(3), -11.0(3), 179.5(3)	+36.3	[74]
$[Ni(L^9)_2(N_3)_4]\cdot H_2O^h$	(**9**)	101.6(1)	3.274(1)	2.039(3), 2.184(3)	-179.8(2), 2.0(1)	+22.8	[62]
$[Ni(L^{10})_2(N_3)_4]^i$	(**10**)	103.7(1)	3.448(1)	2.217(4), 2.169(4)	-178.4(2), 8.9(9)	+23.35	[75]
$[Ni(L^{11})_2(N_3)_4]^j$	(**11**)	98.98(5)	3.2362(3)	2.1598(12), 2.0964(12)	89.57(5), -87.57(5)	+18.61	[64]
$[Ni(L^{12})_2(N_3)_4]^k$	(**12**)	98.36(9)	3.2394(4)	2.192(2), 2.087(2)	89.2(1), -89.4(1)	+31.87	[64]
$[Ni(L^{13})_2(N_3)_4]^l$	(**13**)	100.73	3.2511(6)	2.136(3), 2.085(3)	179.0(1), -7.0(1)	+33.73	[76]
$[Ni(L^{14})(N_3)_4]^m$	(**14**)	101.7(2), 101.1(2) (101.4)	3.330(1)	2.152(6), 2.150(6), 2.144(6), 2.159(6)	-177.5(3), 1.0(2), -177.2(3), 3.0(2)	+20.96	[77]

[a]L^2 = condensation product of 2-benzoyl pyridine and triethylenetetramine; [b]L^3 = *N*,*N*-bis(2-pyridylmethyl)amine;[c] L^4 = *N*-(2-pyridylmethyl)-*N*′,*N*′-diethylethylenediamine; [d]L^5 = *N*,*N*-dimethyl-*N*′-(pyrid-2-ylmethyl)-ethylenediamine; [e]L^6= 2-[(2-hydroxypropylimino)methyl] phenol; [f]L^7 = bis(2-(3,5-dimethyl-1H-pyrazol-1-yl)ethyl)amine; [g]L^8= *N*′-(2-pyridin-2-ylethyl)pyridine-2-carbaldimine; [h]L^9 = 2,2′:6′,2″-terpyridine; [i]L^{10} = methylbis-(3-aminopropyl)amine;[j] L^{11} = *N*,*N*-diethyl-*N*′-((3,5-dimethyl-*1H*-pyrazol-1-yl)methyl)ethane-1,2-diamine; [k]L^{12} = *N*-((*1H*-pyrazol-1-yl)methyl)-*N*′,*N*′-diethylethane-1,2-diamine; [l]L^{13} =1-Methyl-2-[o-(thiomethyl)phenylazo]imidazole; [m]L^{14} = prepared from the reaction of 2-benzoylpyridine with *N*,*N*′-bis-(3-aminopropyl)ethylenediamine.

Table 4. Values of J_{calc}, (cm^{-1}) calculated with different DFT functionals and formulas (1)−(3)

DFT functional	J_{calc}, cm^{-1}		
	Ruiz, (2)	Yamaguchi, (3)	Noodleman, (1)
B3LYP	27.3	40.9	40.9
B3LYP*	20.5	30.8	30.8
PBE0	29.3	43.9	44.0
TPSSh	25.3	37.9	37.9

Table 5. Mulliken spin populations (ρ) and total charges (q) on atoms of the exchange fragment (B3LYP*/6-311G(d,p)) in high (HS) and low spin states (BS)

Spin state	Ni1A		Ni1B		N1Z		N4Z	
	ρ	q	ρ	Q	ρ	q	ρ	q
HS	1.629/1.360		1.653/1.372		0.025/-0.764		0.015/-0.726	
BS	1.633/1.361		-1.656/1.372		-0.012/-0.764		0.000/-0.725	

Scheme captions

Scheme 1. The most common coordination modes of bridging azido ligands to Ni(II) (end-to-end (μ-$_{1,3}$-N_3) and end-on (μ-$_{1,1}$-N_3)).

Scheme 2. Synthesis of ligand **HL**Cl and complex **1**

Figure captions

Figure 1. Graphical representation of **1**. Non-coordinated water and methanol molecules have been left out for clarity.

Figure 2. Temperature dependences of χT and inverse susceptibility. Solid line is the best fit of the experimental data using eq. 4 and Curie-Weiss law.

Figure 3. Relative stability ΔE (kcal mol^{-1}) of **HL**Cl isomers in vacuum and methanol.

Figure 4. Shape of the localized magnetically active SOMOs of the complex **1** (grey spheres – carbon, blue – nitrogen, red – oxygen atoms, cyan – nickel; trimethylammonium group is removed for clarity, contour value is 0.04 e·Å^{-3}).

Figure 5. SD in the BS state of complex **1** (pink and magenta surfaces – α and β spin, contour value 0.02 e·Å^{-3})

Table captions

Table 1. Crystal data and structure refinement details for **1**.

Table 2. Selected bond lengths (Å) and angles (°) for **1**.

Table 3. Structural and magnetic parameters of related bis(μ-$_{1,1}$-azido) bridged Ni(II) complexes

Table 4. Values of J_{calc}, (cm^{-1}) calculated with different DFT functionals and formulas (1)−(3)

Table 5. Mulliken spin populations (ρ) and total charges (q) on atoms of the exchange fragment (B3LYP*/6-311G(d,p)) in high (HS) and low spin states (BS)

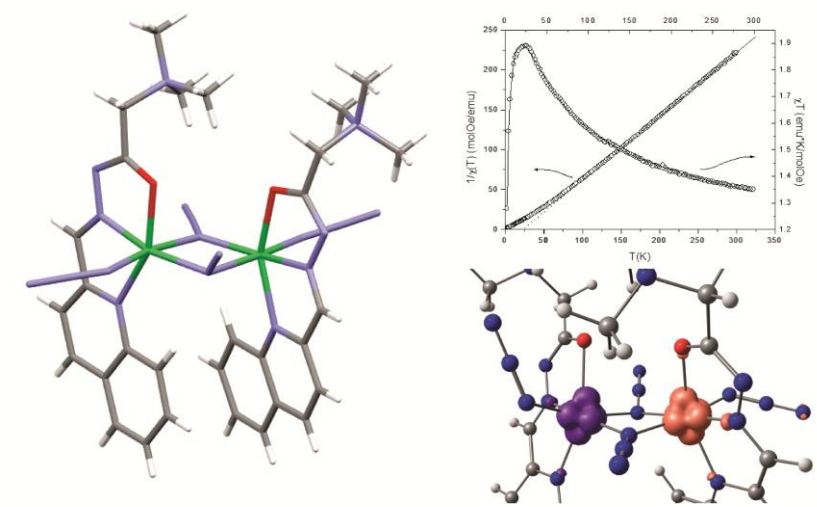

Synthesis, characterization and magnetic properties of dinuclear double end-on azido bridged Ni(II) complex with the condensation product of 2-quinolinecarboxaldehyde and Girard's T reagent. DFT-BS explanation of ferromagnetic exchange coupling in dinuclear Ni(II) complex.